Fusion Engineering and Design 220 (2025) 115310

Contents lists available at ScienceDirect

Fusion Engineering and Design

journal homepage: www.elsevier.com/locate/fusengdes

Tests of power supply and fast discharge unit for the Frascati Coil Cold Test Facility

A. Lampasi [a,b,*], M. Manganelli [a,b], S. Pipolo [a,b], R. Romano [a,b], B. Taheri [a], P. Zito [a,b]

[a] National Agency for New Technologies, Energy and Sustainable Economic Development (ENEA), Frascati, 00044 , Italy
[b] DTT S. c. a r. l., Frascati, 00044 , Italy

ARTICLE INFO

Keywords:
Superconductors
Cold tests
Coil power supply
Quench protection
Fast discharge units
Silicon carbide varistors

ABSTRACT

Cold test facilities are essential for the advancement of fusion energy research. The Frascati Coil Cold Test Facility (FCCTF) was envisioned to test DTT superconducting coils at cryogenic temperature and full current. The FCCTF is also useful for early optimization and validation of other key technologies such as power supply (PS), quench detection system and protection fast discharge unit (FDU).

The PS is rated 44 kA with 24-pulse topology to meet the requirement for low current ripple even for a single load coil. The FDU design is based on a fully static breaking mechanism and on nonlinear varistors for energy dissipation. The FDU can be configured to comply with all possible requirements of central solenoid, toroidal field and poloidal field coils in terms of current, peak voltage, discharge time and energy dissipation.

This paper presents the FCCTF design and the most relevant acceptance tests performed on its PS and FDU, showing that they are suitable for their purpose.

1. Introduction

The Divertor Tokamak Test (DTT) facility is under construction in the ENEA research center in Frascati, Italy (Fig. 1) [1]. The main scope of the DTT experiments, within the framework of the EUROfusion Roadmap [2], will be the study of heat exhaust and the development of solutions for DEMO and future commercial reactors. DTT will include 18 toroidal field (TF) coils in Nb_3Sn, 6 central solenoid (CS) modules in Nb_3Sn, 2 poloidal field (PF) coils in Nb_3Sn (PF1/6), 4 PF coils in NbTi (PF2–5) and some spare and prototype coils [1,3]. In practice, each of these coils, in particular those based on Nb_3Sn, can be considered as a first-of-a-kind manufacturing and should be qualified and characterized [4].

Cold test facilities are crucial in the development and validation of superconductors in forms of cables, joints, assemblies or coils. While SULTAN [5] has a fundamental role for many cables and joints, some facilities were specifically conceived for coils in fusion experiments [6–10]. These facilities are essential for the advancement of fusion energy research, ensuring reliability, performance and stability under the operational conditions.

As part of the DTT project, to minimize risks associated with manufacturing and to support the development of relevant fusion technologies, it was decided to test most of superconducting coils before final assembly. For this purpose, the Frascati Coil Cold Test Facility (FCCTF) was established very close to the DTT site (see Fig. 1) to test the superconducting coils at cryogenic conditions (4.2 K) and full operational current (up to 42.5 kA).

The FCCTF is also useful to verify other key fusion technologies such as power supplies (PSs), quench detection and protection systems [11]. The requirements for a PS system associated with a superconducting test facility are not trivial. The current should be steady state and able to sustain different ratings (42.5 kA for DTT TF coils, in the range of 28–34 kA for the CS and PF coils) with a low ripple even at the lowest current level. The PS voltage cannot be low like in a cable test facility because it should sustain ramps on high inductances and the drops on connections such as room-temperature busbars. Specifications of 44 kA, 100 V and 24-pulses were selected for the FCCTF PS [12].

Superconducting coils need also a fast discharge unit (FDU) to protect them against fault events such as quenches [13]. A FDU can be outlined as a circuit breaker in series with the PS and the load coil. The circuit breaker is normally closed to carry the coil current, but it can be opened to divert this current into a dissipative element like a resistor in

* Corresponding author.
E-mail address: alessandro.lampasi@enea.it (A. Lampasi).

https://doi.org/10.1016/j.fusengdes.2025.115310
Received 26 January 2025; Received in revised form 20 May 2025; Accepted 29 June 2025
Available online 12 July 2025

Fig. 1. Aerial view of ENEA Frascati research center including the DTT and the FCCTF areas.

order to discharge the energy stored in the coil.

In a test facility for superconductors, the FDU is not only a safety tool, but it is often operated on purpose as part of the procedure, for example to calibrate the detection or to estimate AC losses. Therefore, the FDU must ensure a high quantity of operations and an acceptable recovery time for a new test. For the first time in nuclear fusion applications [13, 14], the FDU for the FCCTF will have a fully electronic, without mechanical components, and redundant static circuit breaker (SCB) [12]. The energy stored in the coil will be absorbed by nonlinear silicon-carbide (SiC) varistors instead of resistors. The connection of the banks of dump varistors can be adapted to absorb the energy of each TF, CS or PF coil (ranging from 40 MJ to 250 MJ) without exceeding its maximum peak voltage [3].

This paper presents the most relevant acceptance tests performed on the PS and FDU for the FCCTF, showing that they are suitable for their purpose.

2. The FCCTF test program

Fig. 2 shows a 3D view of the FCCTF. The FCCTF cryostat can accommodate magnets up to 7 × 3 × 1.7 m (length, width and height), having a maximum weight of 17 tons. It is supported by a supercritical helium refrigerator with a mass flow rate of 73 g/s and an inlet temperature of 4.5 K, a vacuum system achieving pressures below 10^{-5} mbar. This setup was optimized to test all the DTT Nb_3Sn coils at their maximum current values. The dimensions of the coils can be seen in Fig. 3. In Fig. 2a TF coil is placed close to the cryostat to show the available space.

Instrumentation and magnet signals will be acquired and monitored

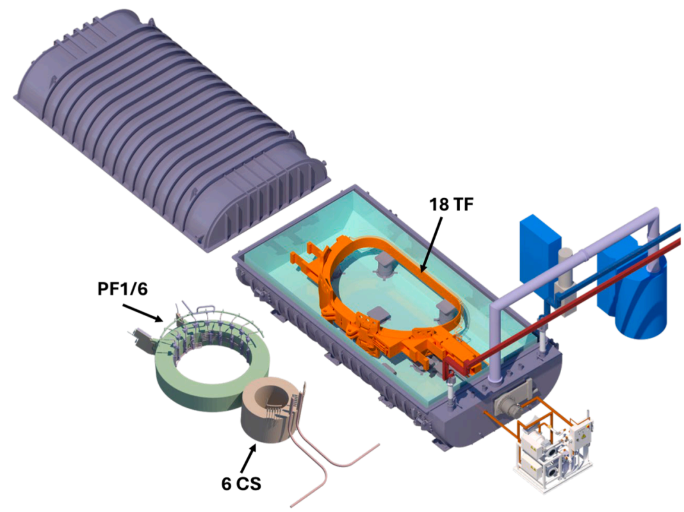

Fig. 3. Schematic view of the positioning of the different DTT coils inside the cryostat.

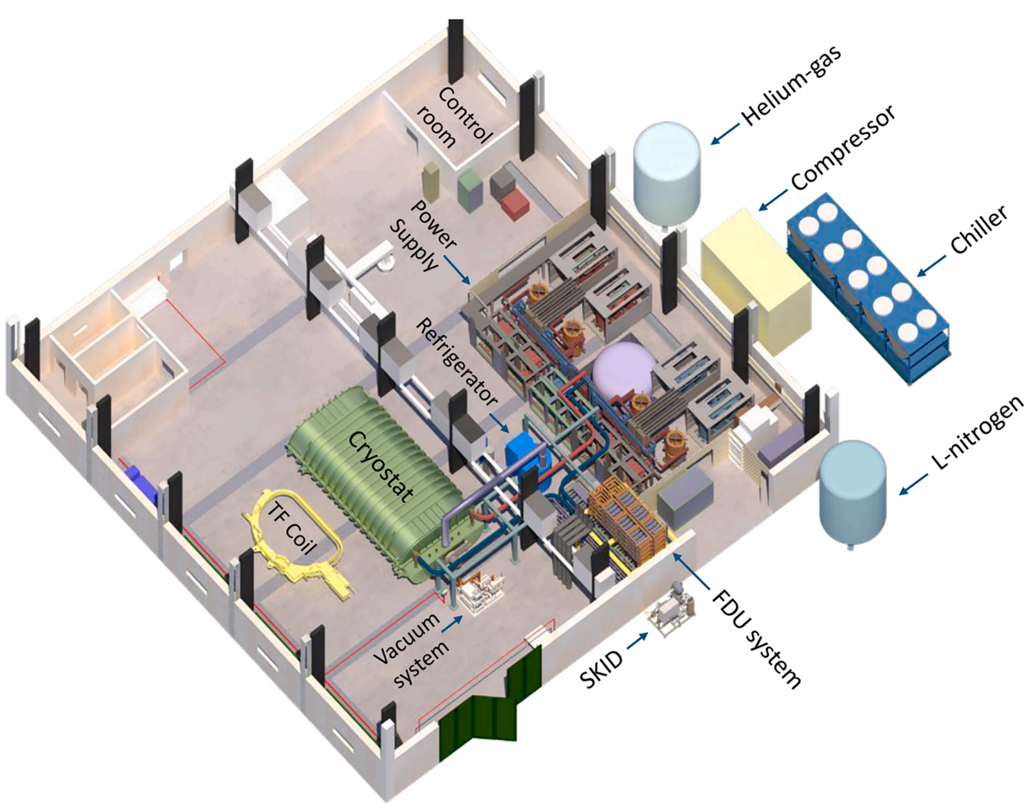

Fig. 2. 3D view of the layout of the FCCTF.

remotely through the CoDAS (Control and Data Acquisition System). The CoDAS will be tested in a simplified version compared to the full DTT system, incorporating the quench detection system.

During the test, the DTT coils will be evaluated for electrical integrity at cryogenic temperatures by energizing them to their operational current with a ramp rate below 100 A/s, accounting for the voltage at the coil terminations caused by the self-inductance of a single coil. The current will then be maintained steady at the operational level for approximately one hour while the helium inlet temperature is gradually increased using a heater positioned upstream of the inlets.

During the cold tests, a quench is detected when the voltage across the two ends of a double pancake (typically zero under normal operating conditions), exceeds the threshold value of 100 mV and remains above this level for >500 ms. Of course, one of the scopes of the tests is to refine this algorithm. Once a quench is detected, the quench protection system is activated, safely discharging the coil energy through the FDU. While this discharge follows an exponential decay in standard FDUs, the varistors induce a different curve [15] that will be studied and optimized in the FCCTF.

The test will also assess superconducting performance, thermo-hydraulic characteristics, and the behavior and resistance values of joints and terminations of the coils.

3. Acceptance tests on the PS

3.1. Structure of the PS

The FCCTF PS is in practice the PS for the 18 DTT TF coils in series, manufactured by the Spanish company JEMA. The structure of the PS is schematized in Fig. 4.

After the safety AC circuit breaker at 20 kV, the three-phase input line is distributed to four 20kV/100 V transformers. The transformers have extended-Δ windings to implement a full 24-pulse configuration while exhibiting a uniform impedance towards the input grid.

The assembled PS underwent factory acceptance tests (FATs) in JEMA premises and further site acceptance tests (SATs) are going after delivery and installation in the FCCTF. Most of the FATs on single components (transformers, DC smoothing reactors, etc.) cannot be presented in this paper for the sake of brevity. Only some key results of the crowbar qualification are reported in the following.

3.2. Crowbar acceptance tests

Fig. 5 details the structure of the crowbar that is only sketched in Fig. 4. The device implements a switch able to freewheel the load current when necessary. The crowbar consists of the parallel of 6 thyristors, a mechanical switch and a ZnO varistor. The ZnO varistor can automatically bypass a fast front of overvoltage. The thyristors are the normal way to activate the crowbar. The closing of the mechanical switch is slower, but, when completed, the current can flow for a very long time.

The crowbar is the only component in the PS classified as safety important, because it must sustain the current in case of faults including an earthquake. Therefore, special tests were requested for the crowbar.

The crowbar must be capable of carrying the rated PS current and withstand the energy throughput (I^2t) during the discharge in case of faults and FDU interventions. According to the specifications, the crowbar must sustain a I^2t of at least 7.2 GA^{2}s that is the maximum

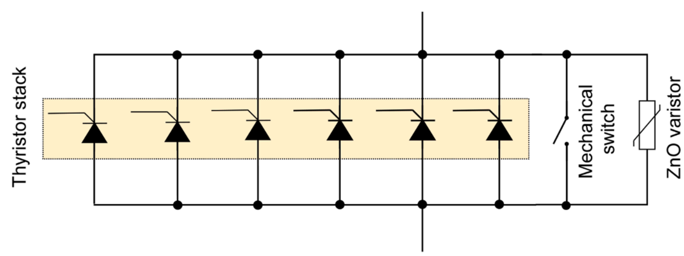

Fig. 5. Basic scheme of the TF crowbar.

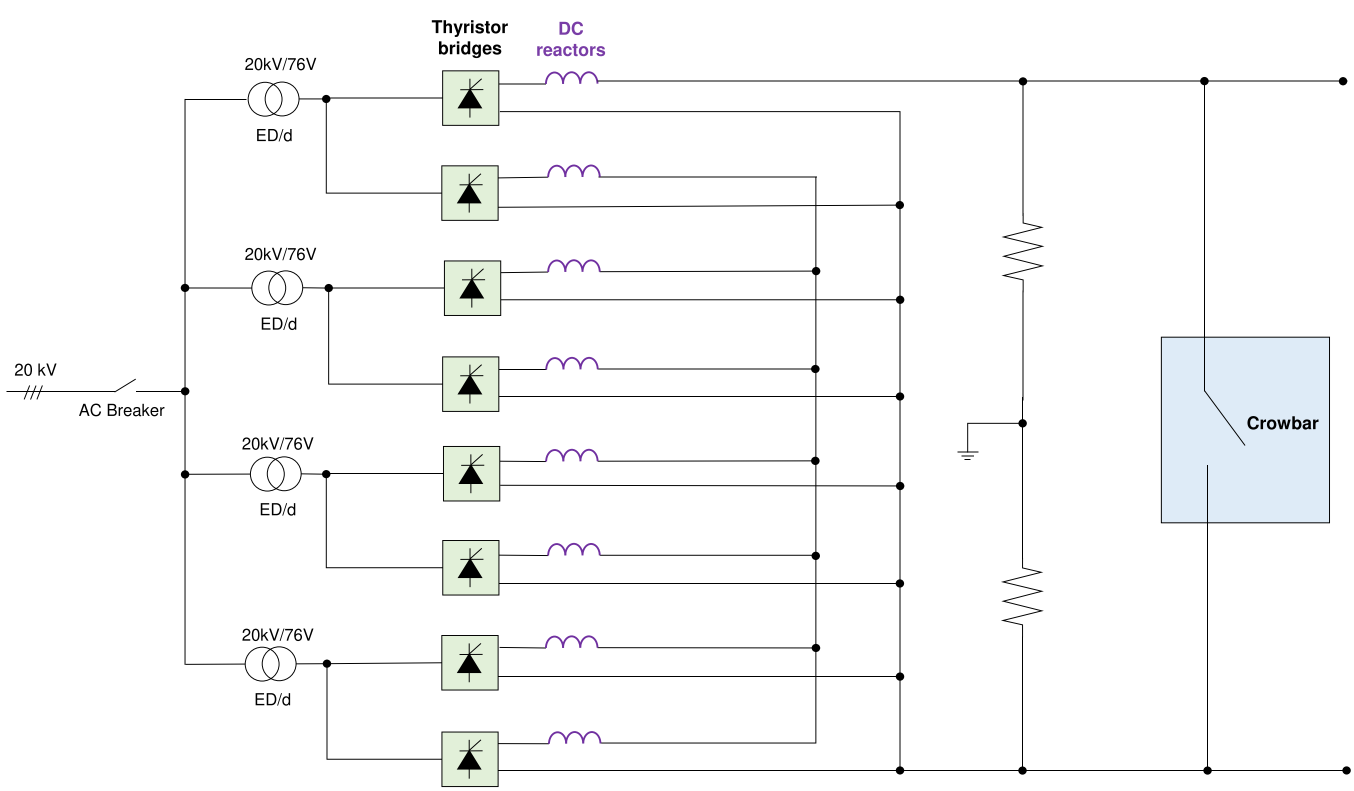

Fig. 4. Basic scheme of the TF PS. Each green block is a standard bridge with 6 thyristors.

expected in the TF coils [12]. Fig. 6 and Fig. 7 present the result of a test at full current to validate its capability of diverting the load current and withstand the resulting I^2t. Moreover, the design was redundant, so 5 thyristors or the mechanical switch are sufficient to carry the specified peak current and I^2t.

To demonstrate that the crowbar can withstand earthquakes, it was seismically tested at Virlab laboratory in Spain as per standard IEC 60068–3–3 [16] using the response spectra estimated for the DTT site. As an example, Fig. 8 shows a biaxial test demonstrating that the crowbar can withstand test response spectra (TRS), measured by accelerometers on the platform, greater than the required response spectrum (RRS).

3.3. PS temperature rise test

As part of PS FATs, a thermal test was performed to characterize temperature rise and its effect due to permanent load. Fig. 9 shows the temperatures measured on some components during a long-duration test at full current. In particular, the 8 DC reactors (see Fig. 4) were considered the most critical components. As sketched in Fig. 9, the temperatures were monitored in the top and middle part of each reactor. After 5 hours of continuous operations all the components reached the temperature equilibrium at values not exceeding the respective limitations.

3.4. PS power quality

The 24-pulse configuration and the 4 extended-Δ MV/LV transformers were selected also to improve the power quality at the input grid. Before connecting the PS in the FCCTF and then in DTT, this aspect was characterized. The measurements were repeated in short circuit at full (43 kA) and partial (15 kA). Tables 1–3 summarize the main result of this characterization.

4. Acceptance tests on the FDU

As sketched in Fig. 10, the FCCTF FDU is an adaptation (mock-up) of one FDU for the DTT TF circuit [12], manufactured by the Italian company OCEM. The only difference between the mock-up and the DT TF FDU consists in the reduced number of varistors to comply with the required space. This is possible because one coil must be discharged instead of 18. The most relevant tests on the FDU will be presented in the following.

4.1. Acceptance tests on varistors

While SiC varistors are typically shaped as discs, tiled varistors were introduced for the high energy of DTT coils. FCCTF FDU has up to 414 tiles in parallel. The current/voltage characteristics were measured for each single tile. The individual characteristics are necessary because varistors cannot be randomly parallelized but must be matched according to their characteristics. One of the reasons for this precaution is the temperature effect, so some tests were performed to identify the dependance of the characteristics on the temperature [17]. The series connections are less critical but should be designed to adjust the voltage produced at FDU intervention.

The verification of rated energy dissipation on a varistor stack was performed in High Test Energy Laboratory (HTEL) of Metrosil in the UK. A stack was subjected to a square wave current of 1328 A until the worst-case energy of 2672 kJ was reached (see Fig. 11). This energy was applied consecutively 10 times with pauses of 3 hours, as expected in DTT.

The FDU dissipative element is composed by two frames of varistor stacks. The frame containing 32 stacks in Fig. 12 was tested at the augmented current at the independent laboratory KEMA in Germany. Since the focus was on electrodynamic resistance, voltage-current characteristics and thermal behavior, this test was performed in AC. As shown in Fig. 13, a current above 50 kA (rated value plus 20 %) was applied, delivering a total energy of about 92 MJ. The thermal camera picture in Fig. 14 shows that, even above the rated energy, the temperature did not exceed the maximum safety value of 190 °C.

The number of varistors in a frame was selected to be highly redundant. As a principle, the rated energy of varistors used in the FCCTF is at least double the amount of coil energy to be discharged. For example, a single TF coil able to store an energy of 41 MJ is discharged through 576 tiles having total rated energy of 86 MJ, a single 43-MJ CS coil through 828 tiles rated 124 MJ and so on. The good safety margin also reduces the temperature increase and the consequent variations in characteristics [17].

4.2. Acceptance tests of the SCB branches

The SCB consists of 22 identical branches in parallel containing integrated gate-commutated thyristors (IGCTs) with related circuitry. For safety redundancy each branch contains two IGCTs in series with independent commands and a single IGCT can sustain the full reapplied voltage (almost 5.5 kV in the worst case).

Since special IGCTs with low on-state voltage drop were ordered, this was measured by the manufacturer. The two IGCTs in a branch were paired to balance the series voltage. Each branch was individually tested at its nominal current (≈2 kA) and in parallel with the other branches at a reduced current (≈300 A) to verify that the branch imbalance in static conditions was within the specified limit of 10 %. Three openings at significant voltage (≈2.3 kV) were repeated, activating only the single and both the IGCTs in series, to verify the imbalance specification also in dynamic conditions.

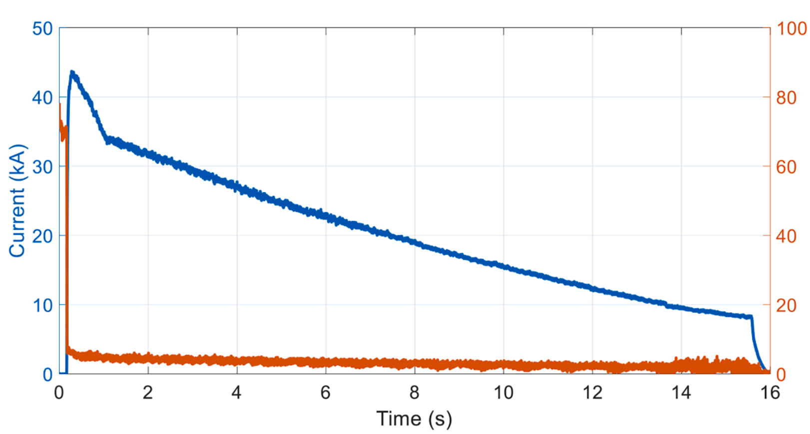

Fig. 6. Crowbar current and voltage after a test of crowbar intervention at full current.

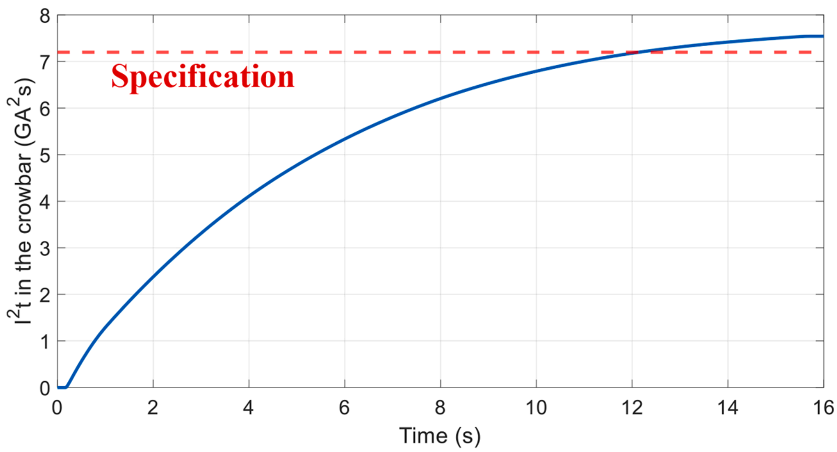

Fig. 7. I^2t passing through the crowbar calculated from the current curve in Fig. 6.

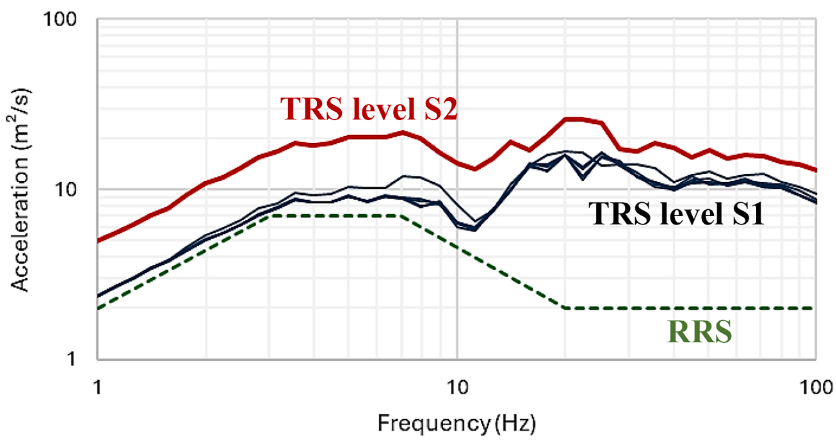

Fig. 8. Example of crowbar TRS compared with the RRS for XZ horizontal.

4.3. Acceptance tests on complete FDU

Due to unavailability of external laboratories able to reach the full value of current of 42.5 kA in DC, the tests on the complete FDU were performed on a scaled version, consisting of one of the three final cabinets connected by a common horizontal busbar. The design of the SCB is modular with 22 identical branches in parallel. The 22 branches are installed in three almost identical cabinets (containing 8 + 8 + 6 branches). Therefore, the test of a SCB cabinet at full current plus 10 % was considered sufficient for acceptance. The resulting maximum value of current is:

$$I_{test} = 1.1 \cdot \frac{8}{22} \cdot I_{rated} = 17 \text{ kA} \tag{1}$$

Another laboratory in KEMA premises was able to generate this current in DC.

Previous experiences with IGCTs in parallel was limited to 8 and for a short time (≪1 s) [18,19], so practically only in dynamic conditions. Hence, the first concern with many IGCTs in parallel was the possible imbalance between branches. The specification was to keep the current imbalance below 10 % both in dynamic and in static conditions. Fig. 15 shows the current measured in all the 8 parallel branches when the test PS is switched on at nominal current. Each branch current reaches the value expected in every DTT FDU (≈2 kA). The static imbalance was evaluated after the transient, resulting <10 %. Similar percentages were found for the dynamic imbalance during current ramp-up (first part of Fig. 15) and ramp-down (see Fig 16).

When the circuit is stable, the SCB was opened to divert the current into the varistor bank. The opening was commanded and synchronized by the local control cubicle (LCC) prepared for the FCCTF. Fig. 16 shows the experimental current and voltage waveforms recorded during a FDU opening at augmented current. The test at 17.4 kA for a cabinet of 8 branches in parallel corresponds to a current of 47.9 kA for the complete SCB (almost 13 % more than the rated current).

Even though the current was scaled, the varistor bank was set to attain the maximum FDU voltage (≈5.5 kV). Like in the FCCTF, a couple of resistors (165 Ω in this case) with a central point connected to ground was inserted in parallel to the varistor to balance the voltage and to detect faults to ground.

The most important performance in the opening phase is the FDU opening time coinciding with the rise time of the voltage across the FDU. As visible in Fig. 16 this opening time is <500 μs, while the DTT requirement was <500 ms. Of course, this enormous reduction was possible when it was decided to pass from an electromechanical or hybrid mechanism [18,19] to a fully static one. This reduction will have a helpful impact on the I^2t [12] and hot-spot temperature [20] of the protected superconductor. Moreover, it will ensure a good breakdown for future DTT switching network units (SNUs) based on the same topology [15].

As shown in Fig. 16, the peak voltage is affected by an overshoot, mainly due to the parasitic inductance in the SCB-varistor loop [21]. This overshoot can be dangerous for the IGCTs (that are already close to their maximum voltage rating), but especially for the superconducting coils (also because the DTT FDU for 6 TF coils will produce almost 1 kV across each single coil [12]). The IGCT snubber and the circuit optimization limit the overshoot to 5.4 kV at augmented current, that is a

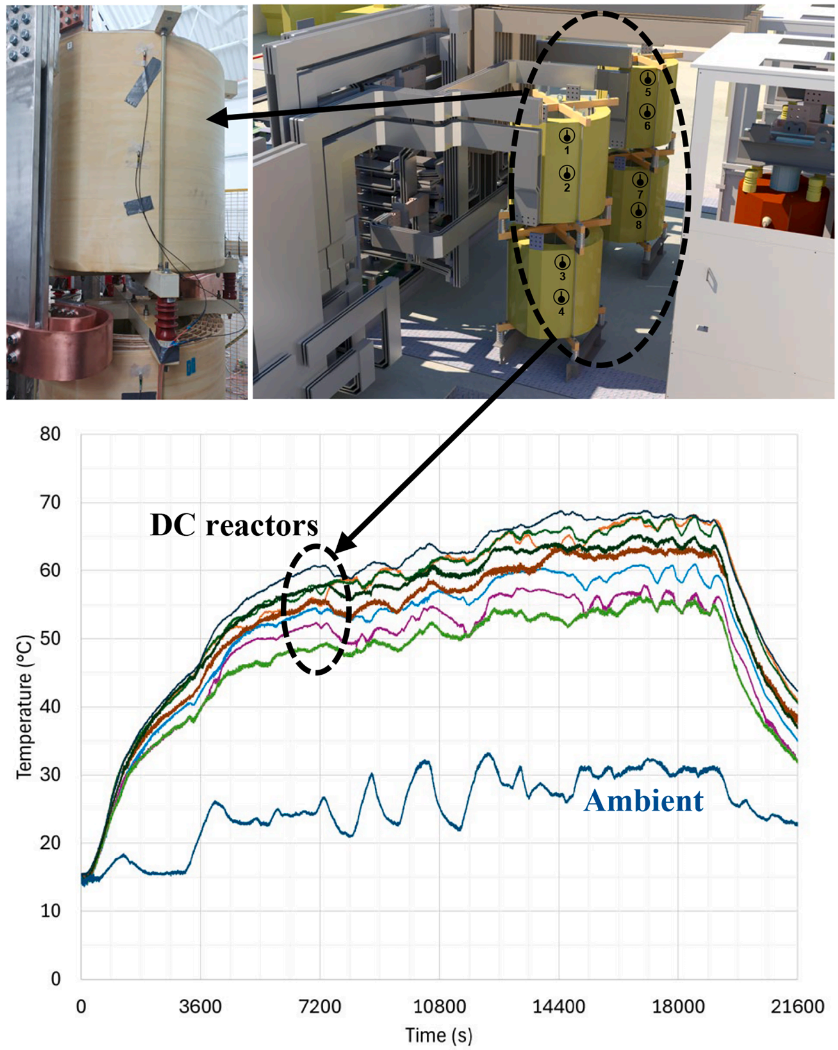

Fig. 9. Temperatures measured on most critical components (DC reactors) during a long-duration test at full current. The temperature probes are placed on the top and middle part of each reactor. The figure refers only to 2 of the 4 columns of DC reactors (see Fig. 4).

Table 1
Measured current THD at partial and full load.

	15 kA	43 kA
Phase L1	4.62 %	4.22 %
Phase L2	3.76 %	3.76 %
Phase L3	3 %	2.41 %

relevant result.

An interesting aspect resulting from tests consists in the moderate dependence of the opening time on the opened current. In JT-60SA, for the parallel of 8 IGCTs, the opening time during the acceptance tests passed from ≈80 μs at 20 kA to ≈400 μs at 1.3 kA [19]. The behavior seems more uniform in Fig. 17, where the voltage curves at opening are compared for different levels of currents (scaled from the tests at one cabinet like in Fig. 16). This uniformity is also a good feature for future SNUs [15].

Table 2
Level of harmonics at partial and full load.

	15 kA			43 kA		
Harmonic	L1	L2	L3	L1	L2	L3
3rd	0.445	2.315	1.615	2.565	0.635	2.080
5th	3.380	0.945	1.735	2.605	3.130	0.905
7th	1.410	1.065	0.080	1.565	1.655	0.570
9th	0.310	0.060	0.310	0.380	0.240	0.235
11th	0.250	0.490	0.145	0.620	0.565	0.060
13th	0.325	0.240	0.065	0.380	0.220	0.080
15th	0.190	0.130	0.080	0.050	0.110	0.135
17th	0.000	0.000	0.000	0.000	0.000	0.000

Table 3
Power parameters measured at partial load.

Quantity	Value
Active power *P*	2.7 MW
Reactive power *Q*	1.59 Mvar
Apparent power *S*	1.62 MVA
$\cos \varphi_{L1}$	0.2
$\cos \varphi_{L2}$	0.2
$\cos \varphi_{L3}$	0.1
Power factor	0.16

5. Analysis of circuit safety and reliability

This paper is focused on the functional tests of the PS and FDU components. The activities performed on the failure mode and effect analysis (FMEA) and on the system reliability and availability will be

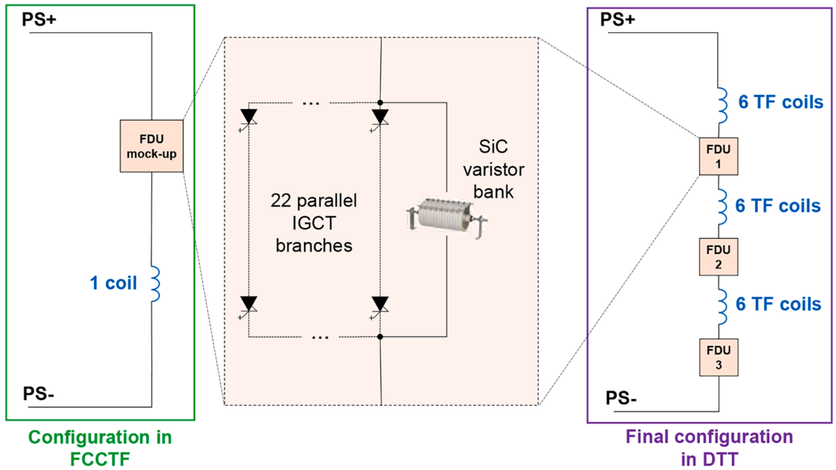

Fig. 10. Comparison between the FDU(s)/coil(s) configurations for the FCCTF and for the DTT TF circuit.

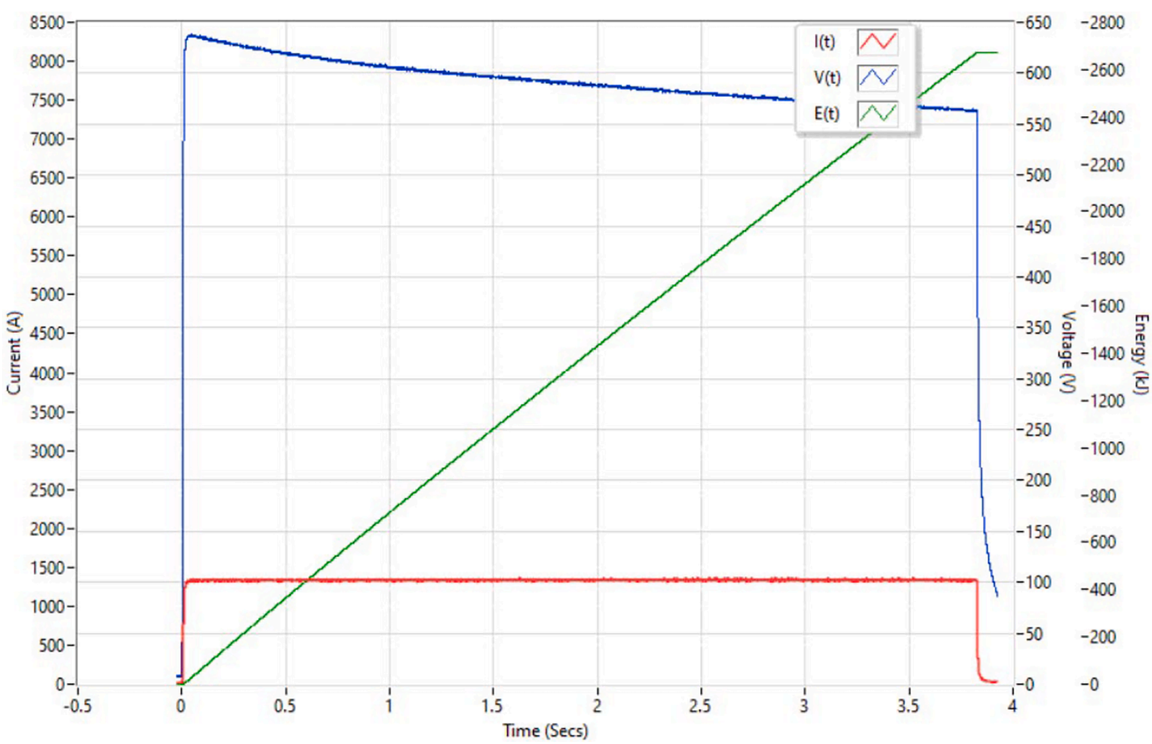

Fig. 11. Thermal test on a varistor stack at HTEL.

presented in a different paper, also extended to the final configuration of the toroidal circuit where the same PS will be in series with 18 coils and 3 FDUs (see Fig. 10) and other contributions will be classified [22]. Nevertheless, it is useful to report some considerations on the safety and reliability of the FCCTF configuration.

The circuit is in a safe state when the SCB is open and the current flows through the varistors. In principle, the crowbar should be closed, but the coil energy could be discharged even with an open crowbar.

The TF PS and FDU are expected to operate in the FCCTF for about 10,000 hours. Considering a possible transfer to DTT after its use in the FCCTF, they could operate for 100 days/year for 25 years, corresponding to about 60,000 hours. These values must be compared to the Mean Time To Failure (MTTF) of the components leading to dangerous events.

For the SCB, the dangerous event is the undesired conduction of at least one of the 22 SCB parallel branches, whereas turning off at least one IGCT in each branch is sufficient to produce the required protective action. For this reason, the IGCT and their control systems are totally redundant and independent. The failure rate (inverse of the MTTF) of a single IGCT is constantly decreasing in the successive through the years [23]. Moreover, it is mainly affected by the permanent DC voltage [24], that is practically negligible in the FDU. Assuming from old manufacturer declarations a very worst-case MTTF≈6600,000 [23] for a single IGCT, including the integrated driver, the MTTF of simultaneous failures on two IGCTs in the same branch is about 2×10^{12} hours, well above the expected 10,000 or 60,000 hours of operations. This corresponds to a failure rate well below the target values suggested in [13].

Besides an internal problem with the IGCTs, a missing opening can arise also due to a failure of the control system to propagate the opening command. In fact, the fiber optics transmitting the commands do not affect safety because of the implemented logic (absence of light would open the SCB). The analysis performed on the FDU control system by a specialized consultant according to the IEC TR 62,380 [25] assessed a

Fig. 12. Varistor frame during the test at higher current in KEMA laboratory.

MTTF≈641,000 hours, corresponding to a MTTF≈4×10^{11} hours for the simultaneous failures of both the redundant control systems. Therefore, also after considering the detrimental effect of the control system, the overall MTTF of the SCB is about 3.4×10^{11} hours, still well above the expected 10,000 or 60,000 hours of operations.

A similar analysis can be carried out for the crowbar. The safest state is attained when the crowbar is closed, As the thyristors in the stack are triggered by 6 independent drivers and are rated to operate even without one of them, it is critical when two thyristors are not activated. The MTTF of a single thyristor (but operating at higher voltage) is about 10^7 hours, leading to a MTTF≈3×10^{12} hours for the whole rack, that is in the same order of the redundant IGCTs. Considering also the presence of the mechanical switch, the crowbar reliability practically coincides with that of the control system.

The calculations are more complex for the final circuit with 3 FDUs (see Fig. 10). However, simulations performed with the technique in [20] showed that the discharge is effective even when only two FDUs success to open.

Finally, it is important to stress that the completely static FDU switch allows more and faster qualification tests with respect to other solutions, also following the guidelines in [13], including the possibility of performing periodic tests even at high current during operations. This should reasonably improve overall reliability and availability.

6. Conclusions

The FCCTF is crucial for the progress of DTT and in general of the research on magnetic-confinement fusion. The challenging

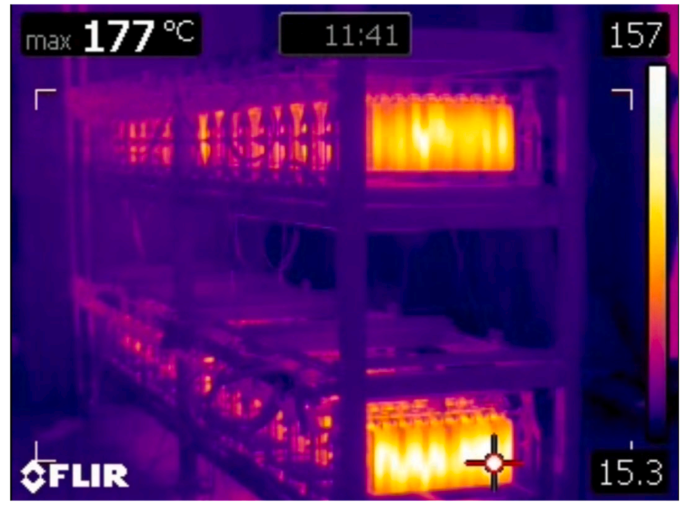

Fig. 14. Temperature distribution, measured by thermal camera, on the stack in Fig. 12 at the end of the test in Fig. 13.

specifications for the FCCTF PS and FDU required an extensive activity of validation. The acceptance tests on the components demonstrated that the design is suitable for the requirements and provided relevant guidelines for the operations. The most relevant tests and related results were presented in this paper.

In addition to the DTT TF, PF and CS coils, the FCCTF PS and FDU can operate on superconductors with different ratings of current, voltage, discharge time and energy dissipation.

The described PS and FDU are now installed in the FCCTF for integrated tests throughout 2025. The cold tests on superconductors are

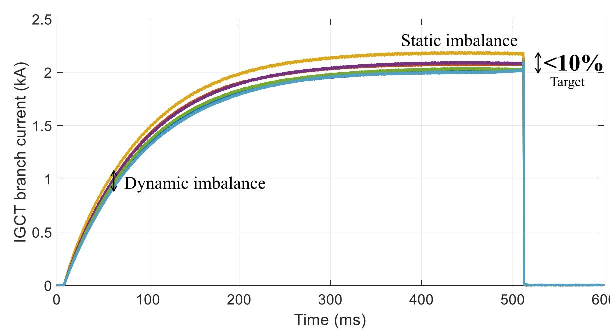

Fig. 15. Current measured in each of the 8 IGCT branches in parallel after the PS is switched on.

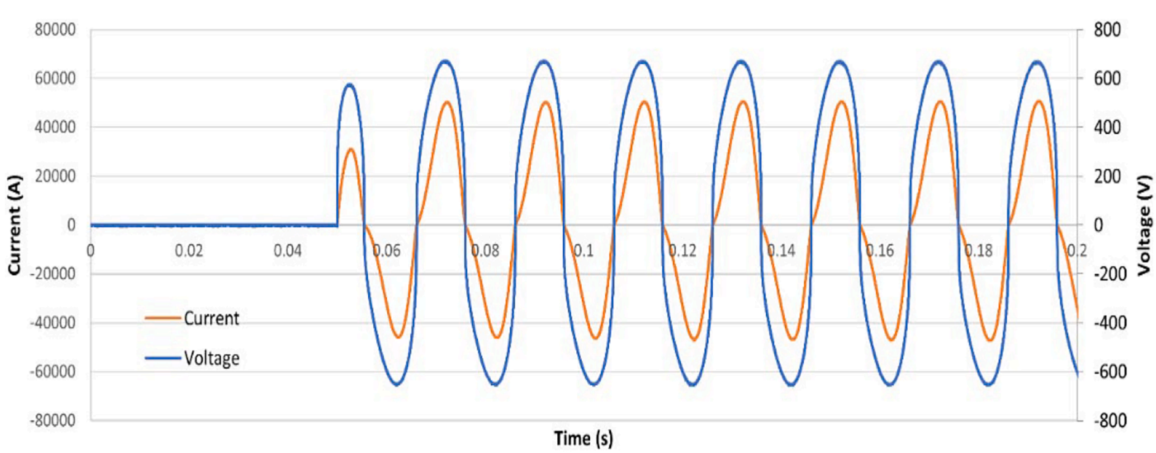

Fig. 13. Waveforms of current and voltage recorded at the KEMA laboratory. The current is not sinusoidal due to the nonlinear effect of varistors.

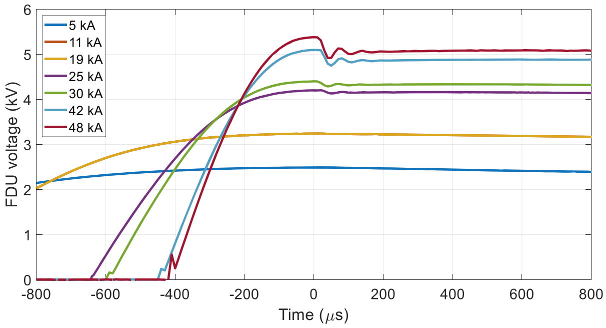

Fig. 16. Current and voltage waveforms recorded during a FDU opening at augmented current. The decay after opening is very fast because the available dummy load was only 7 mH.

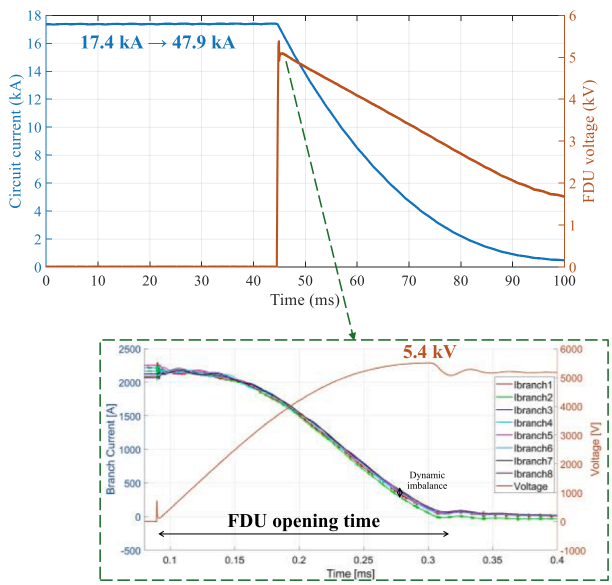

Fig. 17. Comparison of voltage curves measured during tests at different levels of the opened current.

expected to start in 2026.

CRediT authorship contribution statement

A. Lampasi: Writing – original draft, Supervision, Resources, Project administration, Investigation, Funding acquisition, Data curation, Conceptualization. **M. Manganelli:** Writing – review & editing, Writing – original draft, Visualization, Resources, Investigation, Data curation. **S. Pipolo:** Visualization, Validation, Methodology, Data curation, Conceptualization. **R. Romano:** Validation, Supervision, Resources, Conceptualization. **B. Taheri:** Writing – review & editing, Visualization, Validation, Software, Resources, Investigation, Funding acquisition, Formal analysis, Data curation. **P. Zito:** Writing – review & editing, Visualization, Supervision, Project administration, Investigation, Data curation, Conceptualization.

Declaration of competing interest

The authors declare that they have no known competing financial interests or personal relationships that could have appeared to influence the work reported in this paper.

Acknowledgments

The authors acknowledge the staff of JEMA Energy (A. Arenal, A. Dorronsoro, A. Olarte, I. Sorazu, D. Vian) and OCEM Energy Technology (R. Casalini, A. Clos, F. Gherdovich, G. Taddia) for the efforts during the tests and for sharing the measurement data.

The authors acknowledge OCEM Energy Technology and T. Pinna (Eni and DTT) for the discussions on circuit reliability that were partially reported in this paper.

Data availability

Data will be made available on request.

References

[1] F. Romanelli, et al., Divertor Tokamak Test facility Project: status of Design and Implementation, Nucl. Fusion. 64 (11) (2024) 112015. Number.
[2] EUROfusion. European Research Roadmap to the Realisation of Fusion Energy. 2018. Available online: http://www.euro-fusion.org/eurofusion/roadmap/ (accessed on 20 August 2024).
[3] A. Lampasi, C.R. Lopes, M. Manganelli, S. Pipolo, P. Zito, Power Supply Systems for the DTT Superconducting Magnets, in: 21st IEEE Mediterranean Electrotechnical Conference (MELECON 2022), Palermo, Italy, 2022, 14-16 June.
[4] N. Mitchell, et al., Superconductors for fusion: a roadmap, Supercond. Sci. Technol. 34 (10) (2021).
[5] P. Bruzzone, et al., Test of ITER conductors in SULTAN: an update, Fusion Eng. Des. 86 (6–8) (2011) 1406–1409.
[6] W.A. Maksoud, et al., Status of the cold test facility for the JT-60SA tokamak toroidal field coils, Fusion Eng. Des. 96 (2015) 208–211.
[7] T. Golfinopoulos, et al., Building the Runway: a New Superconducting Magnet Test Facility Made for the SPARC Toroidal Field Model Coil, IEEE Trans. Appl. Supercond. (2024).
[8] J. Xue, et al., Manufacture and Test of CRAFT TF Coil 3×3 Mock-Up, IEEE Trans. Appl. Supercond. 34 (2) (2024) 1–6. MarchArt no. 7700206.
[9] E. Ortiz, et al., Commissioning and Operation of ITER CS Module Test Facility: DC Power Supply and DC Breaker Systems, IEEE Trans. Appl. Supercond. 34 (5) (2024) 1–6. AugArt no. 9502106.
[10] ITER (online). Available: https://www.iter.org/node/20687/d-shaped-coils-will-be-tested-4-k (accessed 17 Jan 2025).
[11] E. Gaio, et al., Status and challenges for the concept design development of the EU DEMO plant electrical system, Fusion Eng. Des. 177 (2022) 113052. April.
[12] P. Zito, M. Manganelli, A. Lampasi, S. Pipolo, R. Lopes, Final design of the DTT toroidal power supply circuit, Fusion Eng. Des. 192 (2023) 113595. July.
[13] M. Xu, et al., Discussion on reliability and test number of switches in Tokamak fast discharge units, Fusion Eng. Des. 206 (2024) 114599.
[14] Q. Xu, et al., Preliminary Design and Analysis of Key Switching Components of Switching Network in Fusion Device, IEEE Trans. Plasma Sci. 52 (9) (2024) 3859–3864. Sept.
[15] A. Lampasi, Benefits of high-energy varistors in breakdown and fast discharge units, Fusion Eng. Des. 187 (2023) 113366. Feb.
[16] IEC 60068-3-3, "Environmental testing - Part 3-3: supporting documentation and guidance - Seismic test methods for equipment", 2019.
[17] T. Galvin, A. Lampasi, P. Zito, D. Coll, G. Kirby, Characterisation of SiC Varistors at ambient and elevated temperatures for protection of superconducting magnets, IEEE Trans. Appl. Supercond. 34 (3) (2024) 1–5. Art no. 4702205, May.
[18] A. Maistrello, et al., Experimental qualification of the hybrid circuit breaker developed for JT-60SA quench protection circuit, IEEE Trans. Appl. Supercond. 24 (3) (2014) 1–5. JuneArt no. 3801505.
[19] A. Lampasi, et al., Final tests of the four switching network units procured by the European Union for JT-60SA, Fusion Eng. Des. 124 (2017) 163–168. November.
[20] T. Galvin, A. Lampasi, R. Bonifetto, M. De Bastiani, Multiphysical modelling of superconducting coil discharge through varistors, Fusion Eng. Des. 216 (2025) 115048. July.
[21] A. Maistrello, E. Gaio, L. Novello, M. Matsukawa, K. Yamauchi, Analyses of the impact of connections' layout on the coil transient voltage at the Quench Protection Circuit intervention in JT-60SA, Fusion Eng. Des. 98–99 (2015) 1109–1112. Volumes.
[22] D.N. Dongiovanni, et al., Fusion Components Failure Rate Database, status and evolution, Plasma Phys. Control. Fusion (2025).
[23] E. Tsyplakov, et al., Reliability evaluation of IGCT based on demanding long-term application, in: PCIM Asia 2019; International Exhibition and Conference for Power Electronics, Intelligent Motion, Renewable Energy and Energy Management, Shanghai, China, 2019, pp. 1–5.
[24] ABB Hitachi Energy, Asymmetric Integrated Gate-Commutated Thyristor 5SHY 42L6500, Datasheet (2012).
[25] IEC Technical Report 62380, "Reliability data handbook - Universal model for reliability prediction of electronics components, PCBs and equipment", 2004.